



**HAL**  
open science

## Effect of the Nd content on the structural and photoluminescence properties of silicon-rich silicon dioxide thin films

Olivier Debieu, Julien Cardin, Xavier Portier, Fabrice Gourbilleau

► **To cite this version:**

Olivier Debieu, Julien Cardin, Xavier Portier, Fabrice Gourbilleau. Effect of the Nd content on the structural and photoluminescence properties of silicon-rich silicon dioxide thin films. *Nanoscale Research Letters*, 2011, 6 (1), pp.1-8. 10.1016/j.nimb.2003.11.037 . hal-01139259

**HAL Id: hal-01139259**

**<https://hal.science/hal-01139259>**

Submitted on 3 Apr 2015

**HAL** is a multi-disciplinary open access archive for the deposit and dissemination of scientific research documents, whether they are published or not. The documents may come from teaching and research institutions in France or abroad, or from public or private research centers.

L'archive ouverte pluridisciplinaire **HAL**, est destinée au dépôt et à la diffusion de documents scientifiques de niveau recherche, publiés ou non, émanant des établissements d'enseignement et de recherche français ou étrangers, des laboratoires publics ou privés.

**NANO EXPRESS**

**Open Access**

# Effect of the Nd content on the structural and photoluminescence properties of silicon-rich silicon dioxide thin films

Olivier Debieu, Julien Cardin, Xavier Portier, Fabrice Gourbilleau\*

## Abstract

In this article, the microstructure and photoluminescence (PL) properties of Nd-doped silicon-rich silicon oxide (SRSO) are reported as a function of the annealing temperature and the Nd concentration. The thin films, which were grown on Si substrates by reactive magnetron co-sputtering, contain the same Si excess as determined by Rutherford backscattering spectrometry. Fourier transform infrared (FTIR) spectra show that a phase separation occurs during the annealing because of the condensation of the Si excess resulting in the formation of silicon nanoparticles (Si-np) as detected by high-resolution transmission electron microscopy and X-ray diffraction (XRD) measurements. Under non-resonant excitation at 488 nm, our Nd-doped SRSO films simultaneously exhibited PL from Si-np and Nd<sup>3+</sup> demonstrating the efficient energy transfer between Si-np and Nd<sup>3+</sup> and the sensitizing effect of Si-np. Upon increasing the Nd concentration from 0.08 to 4.9 at.%, our samples revealed a progressive quenching of the Nd<sup>3+</sup> PL which can be correlated with the concomitant increase of disorder within the host matrix as shown by FTIR experiments. Moreover, the presence of Nd-oxide nanocrystals in the highest Nd-doped sample was established by XRD. It is, therefore, suggested that the Nd clustering, as well as disorder, are responsible for the concentration quenching of the PL of Nd<sup>3+</sup>.

## Introduction

Over the last decade, there has been an increasing interest toward nanomaterials for novel applications. One of the challenging fields concerns silicon-compatible light sources which are getting more and more attractive since they can be integrated to microelectronics devices [1]. Amorphous SiO<sub>2</sub> is an inefficient host matrix for the photoluminescence (PL) of Nd<sup>3+</sup> ions since, on the one hand, the absorption cross section of Nd is low ( $1 \times 10^{-20}$  cm<sup>2</sup>) and, on the other hand, the Nd solubility in silica is limited by clustering [2,3], which quenches the PL of the rare earth (RE) ions [4,5]. However, since the discovery of the sensitizing effect of silicon nanoparticles (Si-np) toward the RE ions [6], RE-doped a-SiO<sub>2</sub> films containing Si-np are promising candidates for the achievement of future photonic devices. In such nanocomposites, Nd<sup>3+</sup> ions benefit from the high absorption cross section of Si-np ( $1-100 \times 10^{-17}$  cm<sup>2</sup>) by an efficient

energy transfer mechanism, which enables the PL efficiency of RE ions to be enhanced by 3-4 orders of magnitude offering interesting opportunities for the achievement of future practical devices optically excited. In contrast to Er<sup>3+</sup> ions [6-8], such materials doped with Nd have not been widely investigated and, accordingly, the energy transfer mechanism between Si-np and Nd<sup>3+</sup> ions, and its limitation [9-16]. Several authors have demonstrated that the energy transfer is more effective with small Si-np [10,11]. Seo et al. [11] have observed a decrease of the PL intensity of Nd<sup>3+</sup> ions upon increasing the Si excess, i.e., increasing the Si-np average size. They concluded that only small Si-np which present excitonic states with a sufficient energy band-gap can excite the <sup>4</sup>F<sub>3/2</sub> level of Nd<sup>3+</sup> ions. Several groups, which studied the effect of the Nd concentration in the PL properties of Nd-doped Si-np/SiO<sub>2</sub> demonstrated that the PL of Nd<sup>3+</sup> ions is more efficient at low Nd concentration [12,13].

The object of the present investigation is therefore to characterize the PL properties of nanostructured thin films containing a low concentration of Si excess as a

\* Correspondence: [fabrice.gourbilleau@ensicaen.fr](mailto:fabrice.gourbilleau@ensicaen.fr)  
CIMAP, UMR CNRS/CEA/ENSICAEN/UCBN, Ensicaen 6 Bd Maréchal Juin,  
14050 Caen Cedex 4, France

function of the Nd concentration and the annealing temperature in relation with their microstructures. The Nd-doped silicon-rich silicon oxide (SRSO) thin layers were synthesized by reactive magnetron co-sputtering. Their microstructures were examined using high-resolution transmission electron microscopy (HRTEM), X-ray diffraction (XRD), and Fourier transform infrared (FTIR) spectroscopy. We could notably establish the proper conditions to obtain efficient PL of Nd<sup>3+</sup> but also describe its limitations.

## Experiment

In this study, Nd-doped SRSO thin layers were deposited at room temperature on *p*-type Si wafers by a reactive magnetron RF co-sputtering method that consists in sputtering simultaneously a pure SiO<sub>2</sub> target topped with Nd<sub>2</sub>O<sub>3</sub> chips. The Nd content was monitored by the surface ratio between the Nd<sub>2</sub>O<sub>3</sub> chips and the SiO<sub>2</sub> target. The sputtering gas was a mixture of argon and hydrogen; the latter enables us to control the Si excess of the deposited layers by reacting with oxide species in the plasma [17]. The samples were subsequently annealed at high temperature ranging from 900 to 1100 °C in a dry nitrogen flow.

The composition of the deposited layers was determined by Rutherford backscattering spectrometry, while microstructural analyses were performed using of XRD and HRTEM on samples prepared in the cross-sectional

configuration using a JEOL 2010F (200 kV). The infrared absorption properties were investigated using a Nicolet Nexus FTIR spectrometer at Brewster's incidence.

Room temperature PL measurements were performed using an argon ion laser operating at 488 nm (7.6 W/cm<sup>2</sup>) as excitation source. This excitation wavelength is non-resonant with Nd<sup>3+</sup> ions so that only an indirect excitation of Nd can occur [13,15]. The visible spectra were recorded using a fast photomultiplier (Hamamatsu) after dispersion of the PL with a Jobin-Yvon TRIAX 180 monochromator, while the infrared PL was measured using a Jobin-Yvon THR 1000 monochromator mounted with a cooled Ge detector and a lock-in amplifier to record the near-infrared spectra up to 1.5 μm.

## Results

In this study, we were interested in four Nd-doped SRSO thin films containing the same excess of Si (7 at.%) with various Nd contents ranging from 0.08 to 4.9 at.%.

### Microstructure

Figure 1 shows the FTIR spectrum of the lowest Nd-doped sample as-deposited and a fit with eight Gaussian peaks. Several bands characteristic of amorphous SiO<sub>2</sub> are observed. The two prominent bands at 1236 (red), and 1052 cm<sup>-1</sup> (blue) are assigned to longitudinal optical

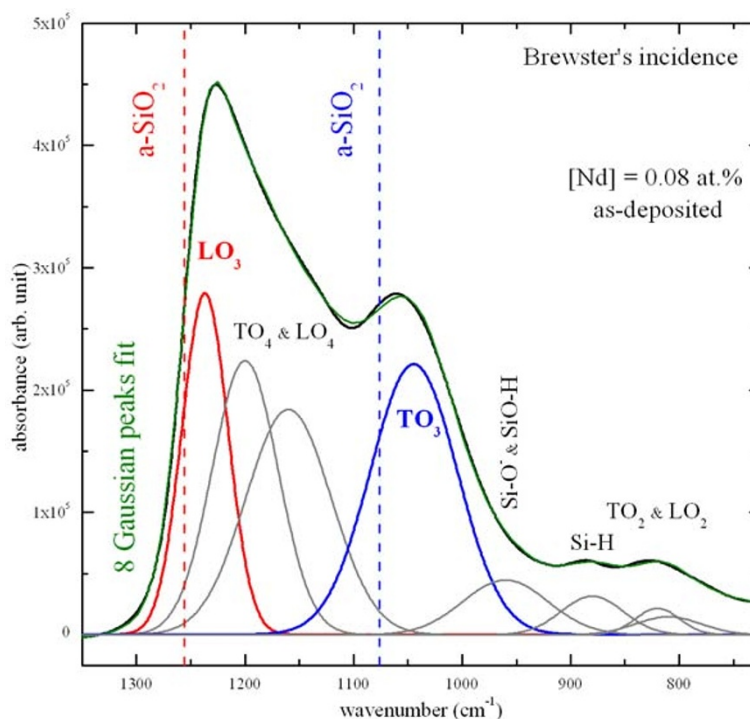


**Figure 1** FTIR spectrum of the lowest Nd-doped sample as-deposited.

( $LO_3$ ) and transverse optical ( $TO_3$ ) phonons of Si-O bonds, respectively. One can notice that these two bands are slightly shifted to lower wavenumbers compared to the stoichiometric positions of a-SiO<sub>2</sub> at 1256 and 1076 cm<sup>-1</sup>, respectively. The  $TO_2$ ,  $LO_2$ ,  $LO_4$ , and  $TO_4$  vibration modes are also present at 810, 820, 1160, and 1200 cm<sup>-1</sup>, respectively. In addition to Si-O vibration modes, a weak absorption band centered at 880 cm<sup>-1</sup> is observed. This peak, which is assigned to Si-H bonds, disappears after annealing because of the hydrogen desorption.

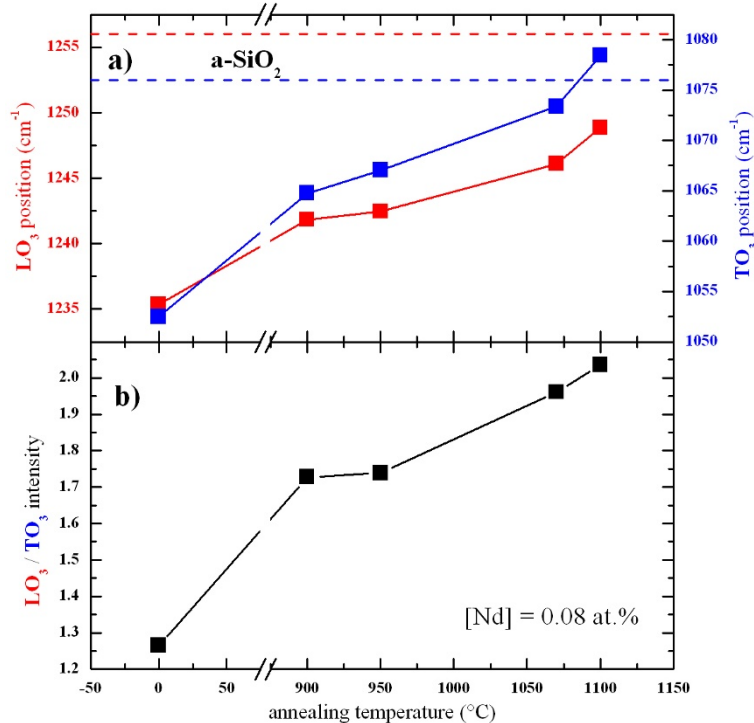
Figure 2a shows the evolution of the positions of the  $LO_3$  and  $TO_3$  vibration modes, and the  $LO_3/TO_3$  intensity ratio, as a function of the annealing temperature. One can observe that, while the annealing temperature was increased, the  $TO_3$  and  $LO_3$  peaks' positions progressively shifted to higher wavenumbers toward their respective stoichiometric positions. It is explained by the phase separation that results in the formation of Si-np [18,19]. The increase of the  $LO_3$  band intensity (see Figure 2b) is related to the increase of the number of Si-O-Si bonds at the SiO<sub>x</sub>/Si-np interface [19,20], i.e., the increase of the density of Si-np [21].

Figure 3 presents the evolution of the FTIR spectra of samples annealed at 1100 °C as a function of the Nd concentration. One can observe that the  $LO_3$  band

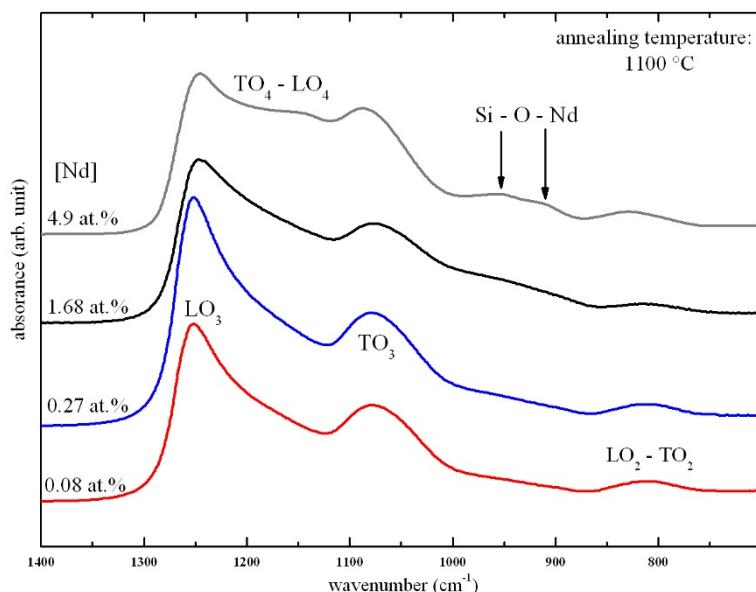
intensity, which is constant at low Nd concentrations of 0.08 and 0.27 at.%, significantly decreased while the Nd content was increased from 1.68 to 4.9 at.%. This evolution contrasts with the one of the  $TO_4$ - $LO_4$  pair modes. Indeed, the  $TO_4$ - $LO_4$  intensity remains constant at low Nd concentrations of 0.08 and 0.27 at.%, and then, it progressively increases with increasing Nd content. This demonstrates that the incorporation of Nd in the thin films generates disorder in the host SiO<sub>2</sub> matrix.

Moreover, one can notice, in the spectrum of the highest Nd-doped sample, the emergence of two weak absorption peaks centered at 910 and 950 cm<sup>-1</sup> which are assigned to asymmetric mode of Si-O-Nd bonds [22]. These peaks are located above a shoulder which can originate from Si-O<sup>-</sup> and Si-OH phonons [23,24]. However, one can exclude the existence of the Si-OH vibration mode after annealing because of the hydrogen desorption. The emergence of these two absorption peaks suggests that other phonons are also optically active in this spectral range.

In Figure 4 is depicted the XRD spectra of the lowest and highest Nd-doped samples. In the former sample, one broad band corresponding to a-SiO<sub>2</sub> is observed, while the pattern of the latter sample indicates the presence of additional phases. In the 27-32° range, it shows various sharp peaks that are located above a broad band



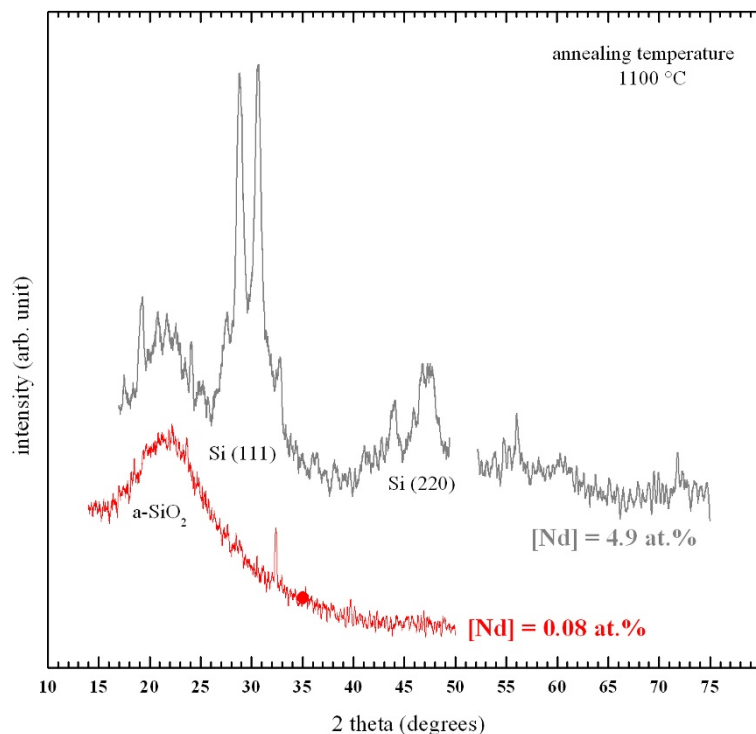
**Figure 2** Evolutions of the positions of the  $LO_3$  and  $TO_3$  peaks, and the  $LO_3/TO_3$  intensity ratio, as a function of the annealing temperature.



**Figure 3** Evolution of the FTIR spectra as a function of the Nd concentration.

centered at  $29^\circ$ . This peak, and the  $48^\circ$  one, indicate the presence of nanocrystalline Si [21,25], while the sharp and intense peaks located at  $27.6^\circ$ ,  $28.8^\circ$ , and  $30.7^\circ$  are assigned to  $\text{Nd}_2\text{O}_3$  crystals. However, the  $28.8^\circ$  peak may result from both crystalline Si and  $\text{Nd}_2\text{O}_3$ . It is interesting to note that the  $27.6^\circ$  and  $30.7^\circ$  peaks fairly

concur with the ones observed in neodymia-silica composites containing  $\text{Nd}_2\text{O}_3$  nanocrystals by several groups [2,3]. As a consequence, the presence of  $\text{Nd}_2\text{O}_3$  and Si nanocrystals in the highest Nd-doped sample is established, while no crystalline phases are detected in the low Nd-doped one.



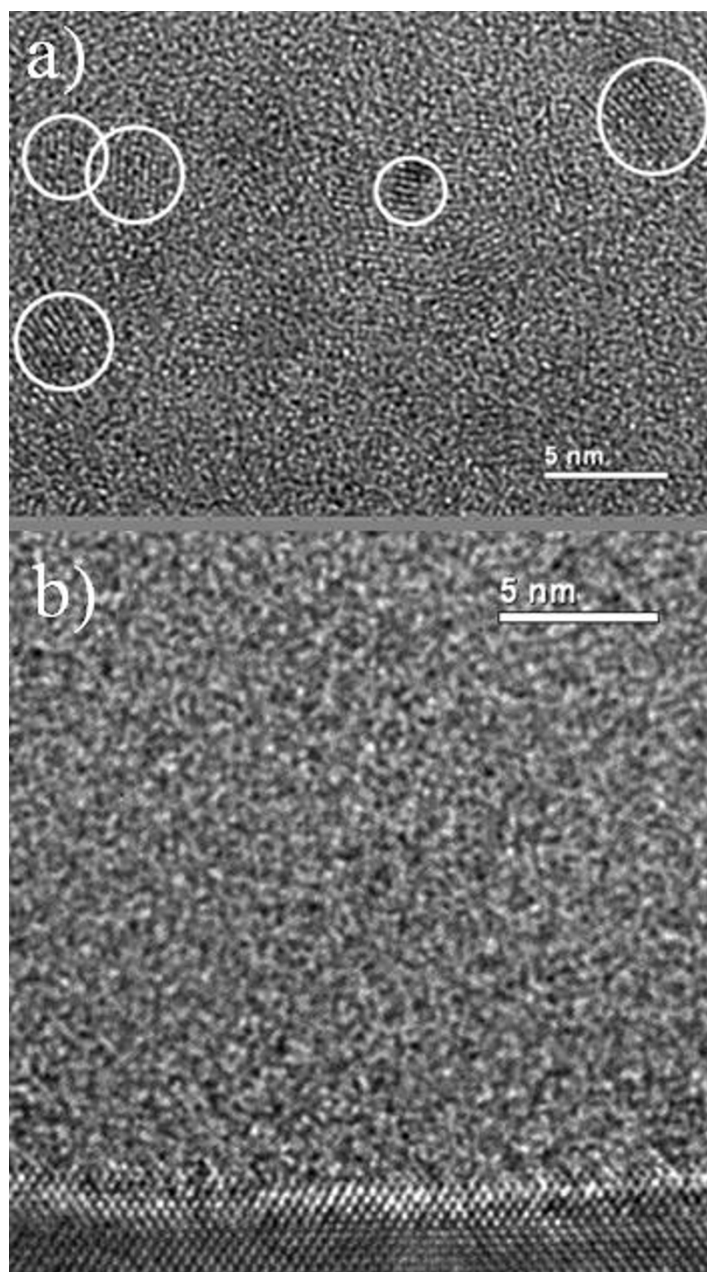
**Figure 4** XRD patterns of the highest and lowest Nd-doped samples annealed at  $1100^\circ\text{C}$ .

Figure 5 shows the HRTEM images of the two latter samples investigated by XRD after annealing at 1100 °C. In the image of the sample with the highest Nd concentration of 4.9 at.% (Figure 5a), one can recognize small Si nanocrystals because of the lattice fringes corresponding to the Si crystalline feature, while no crystalline structure was observed in the images of the film containing the lowest Nd concentration of 0.08 at.% (Figure 5b). These two images are in accordance with the XRD results (see Figure 4). However, one cannot exclude that

the lowest Nd-doped sample could still contain amorphous Si-np.

#### PL spectroscopy

Figure 6 shows the PL spectrum of the lowest Nd-doped sample after annealing at 1100 °C. In the visible domain, one can observe a broad PL band that is originating from quantum-confined excitonic states in small Si-np, while in the infrared domain, three peaks centered at around 920, 1100, and 1350 nm are distinguishable and



**Figure 5** HRTEM images of the highest (a) and lowest (b) Nd-doped samples annealed at 1100 °C.

are attributed to the infra- $4f$  shell transitions of  $\text{Nd}^{3+}$  ions from the  ${}^4F_{3/2}$  level to the  ${}^4I_{9/2}$ ,  ${}^4I_{11/2}$ , and  ${}^4I_{13/2}$  levels, respectively. The presence of the PL of  $\text{Nd}^{3+}$  ions after non-resonant excitation brings to light the sensitizing effect of Si-np towards  $\text{Nd}^{3+}$  ions.

The evolution of the integrated PL intensity of the Si-np PL band and the 920-nm PL peak is shown in the inset of Figure 6. The enhancement of the PL intensity of the broad visible PL band with the annealing temperature is characteristic for Si-np embedded in  $\text{SiO}_2$ . It is due to the increase of the Si-np density, as shown by the increase of the  $\text{LO}_3$  band intensity in the FTIR spectra (see Figure 2) [21], as well as the improvement of their passivation [26] and the decrease of disorder in the host matrix. The latter is a source of non-radiative recombination channels. Interestingly, one can observe that the evolution of the PL intensity of  $\text{Nd}^{3+}$  ions as a function of the annealing temperature is manifestly correlated with the one of Si-np. Reminding that the PL measurements were done under non-resonant excitation, this behavior underlines the strong coupling between Si-np and  $\text{Nd}^{3+}$  ions, and, accordingly, the potential of sensitizing of Si-np. The increase of the PL intensity of  $\text{Nd}^{3+}$  is then explained by the increase of the Si-np density as well as the increase of non-radiative de-excitation channels of both Si-np and  $\text{Nd}^{3+}$ . The  $\text{Nd}^{3+}$  PL intensity is then maximal after annealing at  $1100^\circ\text{C}$  which is generally admitted as the optimal annealing temperature for the PL of Si-np.

Figure 7 shows the behavior of the PL spectra of the thin films annealed at  $1100^\circ\text{C}$  as a function of the Nd concentration. As the Nd content increases from 0.08 to

0.27 at.%, the PL intensity of Si-np drastically drops and disappears at 1.68 at.%. Then, PL of Si-np surprisingly reappears at the highest Nd concentration of 4.9 at.%. Interestingly, one can observe that the positions and widths of the PL peaks of the two lowest Nd-doped samples remain identical (see the inset); whereas the PL peak of the highest Nd-doped film is manifestly shifted to longer wavelengths. According to the quantum confinement model, the PL of the latter sample therefore emanates from Si-np that are sensibly larger than the ones present in the two former samples. In the infrared spectral domain, one can observe that the PL intensity of  $\text{Nd}^{3+}$  ions drops progressively with increasing Nd concentration.

## Discussion

During the annealing, a phase separation occurs as demonstrated in the FTIR spectra in Figure 1, leading to the condensation of Si-np that were detected by XRD (see Figure 4) and HRTEM (see Figure 5). Besides, the presence of Si-np in the films was confirmed by the occurrence after annealing of a 740-nm broad PL band that is characteristic for Si-np.

The presence of PL of  $\text{Nd}^{3+}$  ions under non-resonant excitation evidenced the efficient energy transfer between Si-np and  $\text{Nd}^{3+}$  ions (Figure 6). The concentration quenching of the PL of  $\text{Nd}^{3+}$  ions that was observed in Figure 7 is partly explained by cross relaxation processes between  $\text{Nd}^{3+}$  ions and neighboring  $\text{Nd}^{3+}$  ions and/or  $\text{Nd}_2\text{O}_3$  nanocrystals as reported in glass matrices [4,5]. This is supported by the existence of  $\text{Nd}_2\text{O}_3$  nanocrystals in the highest Nd-doped sample

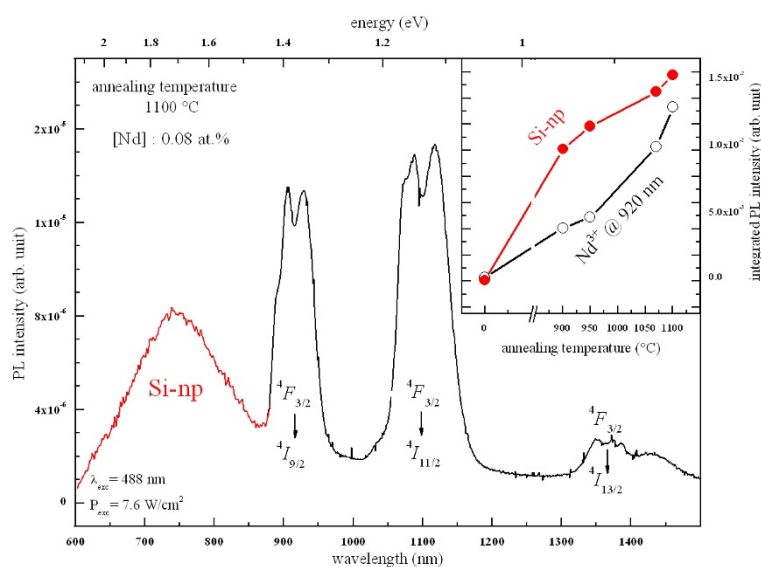


**Figure 6** PL spectrum of the lowest Nd-doped sample annealed at  $1100^\circ\text{C}$ . (Inset) Evolutions of the integrated PL intensity of the Si-np PL band and the first  $\text{Nd}^{3+}$  ions PL peak as a function of the annealing temperature.

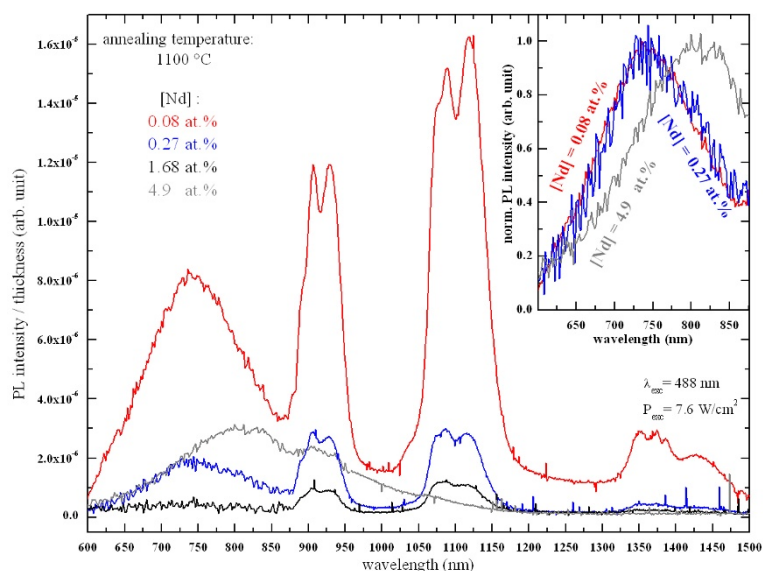


**Figure 7** Evolution of the PL spectra as a function of the Nd concentration.

(see Figure 4). Besides, non-radiative channels inherent to disorder induced by the Nd incorporation (see Figure 3) can be in competition with the energy transfer mechanism between Si-np and  $\text{Nd}^{3+}$  ions in such nano-composite systems leading to the common decrease of the PL intensity of  $\text{Nd}^{3+}$  and Si-np. As a consequence, the emission of  $\text{Nd}^{3+}$  ions is more efficient while Si-np are formed, and while the Nd content is low (0.08 at.%). In such conditions,  $\text{Nd}^{3+}$  ions benefit from the sensitizing effect of Si-np and from the weak competition of non-radiative recombinations in the host matrix. The decrease of the PL of Si-np with increasing Nd content ranging from 0.08 to 4.9 at.% (Figure 7) is explained by the raise of energy transfer between Si-np and  $\text{Nd}^{3+}$  ions (which can be luminescent or not), and by the increase of non-radiative recombinations provided by the increase of disorder as shown in Figure 3. Besides, the presence of a  $\text{Nd}_2\text{O}_3$  phase in the host matrix at the highest Nd content significantly modifies the number of oxygen atoms available to form the silicon oxide host matrix consequently leading to the formation of larger Si-np with a higher density. Besides, the formation of  $\text{Nd}_2\text{O}_3$  nanocrystals results in the rise of the average interaction distance between Si-np and Nd atoms (agglomerated or not) leading to the occurrence of not-coupled Si-np, which therefore enables emission of light in the visible range. This explains the presence of the PL peak of Si-np in the highest Nd-doped sample (Figure 7) which is significantly shifted to longer wavelengths. The fact that XRD pattern of Si nanocrystals, were detected in the latter sample and not in the lowest Nd-doped sample (Figure 4) may also be attributed to the modification of the Si-np size and density.

## Conclusion

The relationships between the composition, the micro-structure, and the PL properties of Nd-doped SRSO thin films that contain the same Si excess were studied. We could establish that the maximum of the PL intensity of  $\text{Nd}^{3+}$  ions was obtained after annealing at 1100 °C which corresponds to the better situation for the achievement of highly luminescent Si-np embedded in  $\text{SiO}_2$ , i.e., containing a small quantity of non-radiative recombination channels. It was demonstrated that the PL of  $\text{Nd}^{3+}$  ions was quenched at high Nd-concentration (4.9 at.%) because of the formation of  $\text{Nd}_2\text{O}_3$  nanocrystals and the occurrence of disorder in the host matrix. The former participates in the concentration quenching mechanism because of cross relaxation processes, while the latter induces the occurrence of new non-radiative channels which are in competition with the energy transfer mechanism between Si-np and  $\text{Nd}^{3+}$  ions.

## Abbreviations

FTIR: Fourier transform infrared; LO: longitudinal optical; PL: photoluminescence; RE: rare earth; Si-np: silicon nanoparticles; SRSO: silicon-rich silicon oxide; TO: transverse optical; XRD: X-ray diffraction.

## Acknowledgements

The authors are grateful to the French Agence Nationale de la Recherche, which supported this study through the Nanoscience and Nanotechnology program (DAPHNES project ANR-08-NANO-005).

## Authors' contributions

OD fabricated the thin films and carried out the optical and microstructural characterizations. XP investigated the films by HRTEM. JC made significant contribution to the optical properties. FG conceived of the study and participated in the coordination and writing of the manuscript. All authors read and approved the final manuscript.



### Competing interests

The authors declare that they have no competing interests.

Received: 24 September 2010 Accepted: 21 February 2011

Published: 21 February 2011

### References

1. Kenyon AJ: Recent developments in rare-earth doped materials for optoelectronics. *Prog Quant Electron* 2002, **26**:225.
2. Kępiński L, Zawadzki M, Miśta W: Hydrothermal synthesis of precursors of neodymium oxide nanoparticles. *Solid State Sci* 2004, **6**:1327.
3. Lal B, Kumar S, Aghamkar P, Rohilla S, Singh D: Structural studies of annealed neodymia-silica composite synthesized by sol-gel technique. *Physica B* 2009, **404**:3452.
4. Caird JA, Ramponi AJ, Staver PR: Quantum efficiency and excited-state relaxation dynamics in neodymium-doped phosphate laser glasses. *JOSA B* 1991, **8**:1392.
5. Jacinto C, Oliveira SL, Nunes LAO, Myers MJ, Catunda T: Normalized-lifetime thermal-lens method for the determination of luminescence quantum efficiency and thermo-optical coefficients: Application to Nd<sup>3+</sup>-doped glasses. *Phys Rev B* 2006, **73**:125107.
6. Kenyon AJ, Trwoga PF, Federighi M, Pitt CW: Optical properties of PECVD erbium-doped silicon-rich silica: evidence for energy transfer between silicon microclusters and erbium ions. *J Phys Condens Matter* 1994, **6**:L319.
7. Franzo G, Iacona F, Vinciguerra V, Priolo F: Enhanced rare earth luminescence in silicon nanocrystals. *Mater Sci Eng B* 2000, **69-70**:335.
8. Gourbilleau F, Levalois M, Dufour C, Vicens J, Rizk R: Optimized conditions for an enhanced coupling rate between Er ions and Si nanoclusters for an improved 1.54- $\mu$ m emission. *J Appl Phys* 2004, **95**:3717.
9. Franzo G, Vinciguerra G, Priolo F: The excitation mechanism of rare-earth ions in silicon nanocrystals. *Appl Phys A Mater Sci Process* 1999, **69**:3.
10. Watanabe K, Tamaoka H, Fujii M, Moriwaki K, Hayashi S: Excitation of Nd<sup>3+</sup> and Tm<sup>3+</sup> by the energy transfer from Si nanocrystals. *Physica E* 2002, **13**:1038.
11. Seo SY, Kim M-J, Shin J: The Nd-nanocluster coupling strength and its effect in excitation/de-excitation of Nd<sup>3+</sup> luminescence in Nd-doped silicon-rich silicon oxide. *Appl Phys Lett* 2003, **83**:2778.
12. MacDonald AN, Hryciw A, Lenz F, Meldrum A: Interaction between amorphous silicon nanoclusters and neodymium ions. *Appl Phys Lett* 2006, **89**:173132.
13. Bréard D, Gourbilleau F, Dufour C, Rizk R, Doulan J-L, Camy P: Spectroscopic studies of Nd<sup>3+</sup>-doped silicon-rich silicon oxide films. *Mater Sci Eng* 2008, **146**:179.
14. Bréard D, Gourbilleau F, Belarouci A, Dufour C, Rizk R: Nd<sup>3+</sup> photoluminescence study of Nd-doped Si-rich silica films obtained by reactive magnetron sputtering. *J Lumin* 2006, **121**:209.
15. Gourbilleau F, Belarouci A, Bréard D, Dufour C, Rizk R: Active emitters based on nanostructured Si. *Int J Nanotechnol* 2008, **5**:574.
16. Podhorodecki A, Misiewicz J, Gourbilleau F, Cardin J, Dufour C: High Energy Excitation Transfer from Silicon Nanocrystals to Neodymium Ions in Silicon-Rich Oxide Film. *Electrochem Solid State* 2010, **13**:K26-K28.
17. Ternon C, Gourbilleau F, Portier X, Voivenel P, Dufour C: An original approach for the fabrication of Si/SiO<sub>2</sub> multilayers using reactive magnetron sputtering. *Thin Solid Films* 2002, **419**:5.
18. Hinds BJ, Wang F, Wolfe DM, Hinkle CL, Lucovsky G: Study of SiO<sub>x</sub> decomposition kinetics and formation of Si nanocrystals in an SiO<sub>2</sub> matrix. *J Non-Cryst Solids* 1998, **227-230**:507.
19. Ono H, Ikarashi T, Ando K, Kitano T: Infrared studies of transition layers at SiO<sub>2</sub>/Si interface. *J Appl Phys* 1998, **84**:6064.
20. Charvet S, Madelon R, Gourbilleau F, Rizk R: Spectroscopic ellipsometry analyses of sputtered Si/SiO<sub>2</sub> nanostructures. *J Appl Phys* 1999, **85**:4032.
21. Gourbilleau F, Dufour C, Levalois M, Vicens J, Rizk R, Sada C, Enrichi F, Battaglin G: Room-temperature 1.54  $\mu$ m photoluminescence from Er-doped Si-rich silica layers obtained by reactive magnetron sputtering. *J Appl Phys* 2003, **94**:3869.
22. Ono H, Katsumata T: Interfacial reactions between thin rare-earth-metal oxide films and Si substrates. *Appl Phys Lett* 2001, **78**:1832.
23. Fidalgo A, Ilharco LM: The defect structure of sol-gel-derived silica/polytetrahydrofuran hybrid films by FTIR. *J Non-Cryst Solids* 2001, **283**:144.
24. Innocenzi P: Infrared spectroscopy of sol-gel derived silica-based films: a spectra-microstructure overview. *J Non-Cryst Solids* 2003, **316**:309.
25. Kapaklis V: Structural characterization of silicon nanocrystals from amorphous silicon oxide materials. *J Non-Cryst Solids* 2008, **354**:612.
26. Garrido B, López M, Pérez-Rodríguez A, García C, Pellegrino P, Ferré R, Moreno JA, Morante JR, Bonafos C, Carrada M, Claverie A, de la Torre J, Souifi A: Optical and electrical properties of Si-nanocrystals ion beam synthesized in SiO<sub>2</sub>. *Nucl Instrum Meth. B* 2004, **216**:213.

doi:10.1186/1556-276X-6-161

Cite this article as: Debieu *et al.*: Effect of the Nd content on the structural and photoluminescence properties of silicon-rich silicon dioxide thin films. *Nanoscale Research Letters* 2011 **6**:161.

Submit your manuscript to a SpringerOpen® journal and benefit from:

- Convenient online submission
- Rigorous peer review
- Immediate publication on acceptance
- Open access: articles freely available online
- High visibility within the field
- Retaining the copyright to your article

Submit your next manuscript at ► [springeropen.com](http://springeropen.com)